Improved Secant-Based Global Flexible Power Point Tracking in Photovoltaic Systems Under Partial Shading Conditions

Anusha Kumaresan, *Student Member, IEEE*, Hossein Dehghani Tafti, *Senior Member, IEEE*, Neha Beniwal, *Member, IEEE*, Naga Brahmendra Yadav Gorla, *Senior Member, IEEE*, Glen G. Farivar, *Senior Member, IEEE*, Josep Pou, *Fellow, IEEE*, and Georgios Konstantinou, *Senior Member, IEEE*

***Abstract*—Flexible power point tracking (FPPT) control algorithms have been introduced in the literature to provide frequency support in low-inertia grid-connected photovoltaic (PV) systems. This is achieved by regulating the PV output power to a power reference obtained from the energy management system. Partial shading of PV arrays is a frequent phenomena that needs to be investigated for FPPT operation of PV systems. This article proposes a simple and improved secant-based global FPPT algorithm that tracks the power reference during partial shading conditions. Guaranteed and fast convergence with flexibility to operate on both sides of the global maximum power point are the main contributions of the proposed algorithm. Experimental validation is carried out to demonstrate the efficacy of the proposed algorithm.**

***Index Terms*—Global flexible power point tracking (FPPT), grid-connected photovoltaic (PV) systems, partial shading, secant method, active power control.**

Manuscript received 18 December 2022; revised 3 April 2023; accepted 3 May 2023. Date of publication 18 May 2023; date of current version 21 June 2023. This work was supported in part by the Republic of Singapore's National Research Foundation (NRF) through the "Distributed Energy Resource Management System for Energy Grid 2.0 " project at the Energy Research Institute at Nanyang Technological University, Singapore, and in part by the Office of Naval Research U.S. under DUNS Code: 595886219. Recommended for publication by Associate Editor D. M. Xu. *(Corresponding author: Anusha Kumaresan.)*

Anusha Kumaresan is with the Energy Research Institute at NTU (ERI@N), Interdisciplinary Graduate Programme, Nanyang Technological University, Singapore 639798 (e-mail: anusha010@e.ntu.edu.sg).

Hossein Dehghani Tafti is with the Department of Electrical, Electronic and Computer Engineering, The University of Western Australia, Perth, WA 6009, Australia (e-mail: hossein002@e.ntu.edu.sg).

Neha Beniwal is with the GE Global Research, New York, NY 12309 USA (e-mail: nsingh341@gmail.com).

Naga Brahmendra Yadav Gorla is with the Indian Institute of Technology Palakkad, Kozhippara 678557, India (e-mail: a0135566@u.nus.edu).

Glen G. Farivar is with the Department of Electrical and Electronic Engineering, The University of Melbourne, Parkville, VIC 3010, Australia (e-mail: gh_farivar@hotmail.com).

Josep Pou is with the School of Electrical and Electronic Engineering, Nanyang Technological University, Singapore 639798 (e-mail: josep.pou@ieee.org).

Georgios Konstantinou is with the School of Electrical Engineering and Telecommunications, University of New South Wales, Sydney, NSW 2052, Australia (e-mail: g.konstantinou@unsw.edu.au).

Color versions of one or more figures in this article are available at https://doi.org/10.1109/TPEL.2023.3277580.

Digital Object Identifier 10.1109/TPEL.2023.3277580

I. Introduction

TO OVERCOME the global issues caused by the overexploitation of fossil fuels, there is a drive towards the use of renewable energy sources for electric power generation [1]. Solar energy emerges as a prominent renewable energy source owing to its abundant availability and the incentives provided for clean electricity generation [2]. The conventional method of extracting power from a solar array is to harness the available maximum power by employing a maximum power point tracking (MPPT) [3].

Many MPPT algorithms have been proposed in the literature for operation under uniform irradiance condition [4], as shown in Fig. 1. They constitute the classical algorithms which have low complexity. Notable examples of such algorithms include, constant and variable step size perturb and observe (P&O) [5], [6] and incremental conductance (IC) [7]. However, in practice, all the PV panels in an array may not receive the same amount of irradiance due to partial shading. Shading on some of the panels can occur due to factors such as passing clouds, shadows of trees, or nearby buildings, etc. A nonuniform irradiance could create multiple peaks in the power-voltage (P-V) characteristics of a PV array. Hence, there is a requirement for MPPTs to be able to track the global maximum power point (GMPP) [8]. Consequently, modifications to the classical algorithms are presented to mitigate their inability of GMPP convergence (e.g., enhanced adaptive P&O in [9], modified hill climbing in [10], and improved IC based on search-skip-judge method in [11]). To improve the order of convergence of tracking the GMPP, as compared to the classical algorithms, intelligence-based algorithms based on fuzzy logic [12] and artificial neural network [13] can be employed. However, the requirements of complex control system and large data for training are disadvantageous. Accordingly, optimization-based algorithms such as particle swarm optimization [14], [15] and grey-wolf optimization [16] are presented in the literature to track the GMPP.

The P-V characteristics are dependent on the environmental conditions, and hence, the GMPP also varies according to the irradiance and cell temperature. Therefore, due to the intermittent nature of solar energy, load-demand mismatch occurs frequently if a global maximum power point tracking (GMPPT)

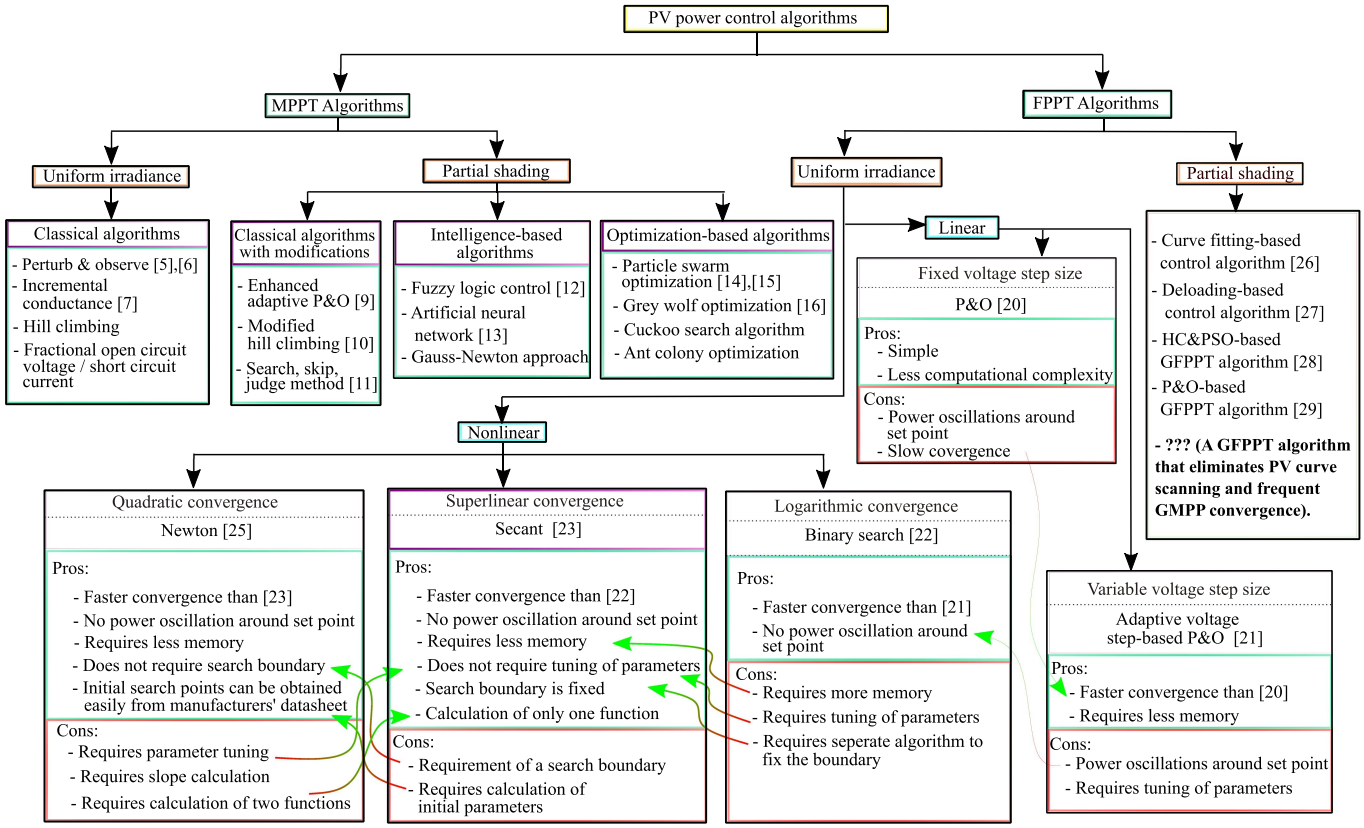

Fig. 1. Overview of PV power control algorithms present in the literature.

algorithm is employed. Consequently, high PV penetration into the power grid can lead to stability issues. The easiest solution is to increase energy storage in the power network to provide inertia, but this comes with an increased cost, space requirement, aging issues and with its own limitation of maximum power handling capacity. Therefore, it is important to look beyond the centralized solutions to resolve the power stability issues and to create an energy market, which is consumer as well as supplier friendly. Hence, a flexible power point tracking (FPPT) control algorithm was introduced in the literature [17], [18], which regulates the PV output power to a desired power reference. This power reference is obtained from the energy management system (EMS) by real time monitoring, operation, and control of the power grid [19].

FPPT is a progressing topic and a few methods have been presented in the literature, as depicted in Fig. 1. The following FPPT algorithms have been proposed for operation under uniform irradiance condition:

Linear search-based algorithms:

1) *Constant voltage step-size:* A P&O-based FPPT algorithm was proposed in [20] that has a low computational complexity. However, the order of convergence is slow.
2) *Variable voltage step-size:* The order of convergence was improved by employing an adaptive voltage-step calculated according to the system parameters in [21].

These linear search-based algorithms suffer from power oscillations around the set point. Moreover, there is a requirement for parameter tuning in adaptive voltage-step-based P&O [21].

To alleviate these issues, nonlinear search-based algorithms are proposed, which are classified further based on their order of convergence in the following:

Nonlinear search-based algorithms:

1) *Logarithmic convergence:* With respect to the nonlinear search algorithms, initially, the binary search-based FPPT algorithm was proposed [22]. The power oscillations are eliminated in this method. However, it requires more memory and tuning of parameters. There is also a requirement of a separate algorithm to set its search boundary.
2) *Superlinear convergence:* A secant-based FPPT algorithm was proposed in [23]. It requires memory of only one variable from the previous instant and the search boundary is fixed. Also, there is no requirement for tuning of parameters. However, some parameters need to be calculated for the initialization purpose of the secant-based FPPT algorithm [24], which is a drawback.
3) *Quadratic convergence:* To eliminate the initial parameter calculation, Newton's method-based FPPT algorithm was proposed in [25]. Only a single initial search parameter is required rather than a search boundary. This initial search point is easily obtained from the manufacturers' datasheet. However, the requirement of derivative for the slope calculation is a drawback.

The mentioned FPPT algorithms operate efficiently only under uniform irradiance. Tracking the power reference becomes challenging during partial shading of the PV modules and a global FPPT (GFPPT) algorithm should be employed. A control

technique using curve fitting was opted in [26] for tracking the power reference during partial shading. However, scanning of data points is required to fit the PV curve and this process needs to be repeated for different PV modules. To avoid this frequent scanning, a GFPPT algorithm based on deloading was presented in [27]. This algorithm converges to the GMPP initially and then, reduces the power gradually to the required power reference, if the power reference is less than the GMPP power. The power is reduced in fixed voltage steps, which makes the convergence slow. To increase the order of convergence, hill-climbing and particle swarm optimization (HC&PSO)-based GFPPT algorithm was proposed in [28]. This algorithm for searches for all the MPPs using the HC algorithm and then, the power reference is tracked using the PSO algorithm. However, the optimization process increases the algorithm complexity and makes it difficult to implement in practical applications. In the stated previous research for partial shading, either frequent scanning of the PV curve is required, or a MPPT algorithm is employed to find the local MPPs (LMPPs). This is a drawback as a large amount of initial data needs to be acquired before the FPPT process commences. Subsequently, the convergence time of these algorithms increases because whenever there is a change in the environmental conditions, the mentioned process has to be carried out to ensure convergence. The P&O-based GFPPT algorithm, recently presented in [29], offers a simple process to converge to the p^* by varying the voltage step in a constant manner. Unlike the GFPPT algorithm based on deloading [27], it does not require the GMPPT convergence to initiate the FPPT process. The GMPPT mode is employed only when the p^* is greater than the GMPP power. However, the convergence process is slow and power oscillations are around the set point. Hence, there is a requirement to develop a GFPPT algorithm that offers fast and guaranteed convergence with minimal amount of initial data.

From the available research on FPPT algorithms for uniform irradiance condition, the secant method-based FPPT algorithm presents promising results with fewer drawbacks. The guaranteed convergence even at the point of inflection by the secant method is the main criteria for choosing this algorithm. All the other algorithms presented in the literature for the uniform irradiance condition halt at the point of inflection when employed during partial shading. This is because either the slope value becomes undefined theoretically, or close to zero during practical implementation, causing the algorithms to choose the wrong path in the subsequent iteration. The superlinear order of convergence (golden ratio - 1.618) is also much closer to the quadratic order of convergence (two) of the Newton's method [30].

Accordingly, this article proposes an improved secant-based (IS-B) GFPPT algorithm that works efficiently during partial shading conditions. The conventional secant method is modified by keeping one of the set points constant while the other changes and converges to the solution [31]. The proposed algorithm is also able to track the power reference on both the left- and the right-side of the GMPP. Though the proposed IS-B GFPPT algorithm is based on the previous work, it addresses one of the biggest challenges of the FPPT algorithms, which is partial shading. In addition, the major contributions of the work are as follows.

1) Fast and guaranteed convergence: The proposed IS-B GFPPT algorithm provides convergence even at the intricate points such as the point of inflection. The intricate points refers to critical points on a P-V characteristic curve where its function is nondifferentiable or the derivative is zero [32]. The derivative at the LMPPs is zero, and the curve is nondifferentiable. Although the conventional secant method has superlinear order of convergence when only a single solution is present, its order is linear when multiple solutions are present [33]. Moreover, in comparison, the proposed IS-B GFPPT algorithm takes fewer steps to converge than the conventional secant method. This is due to the fact that most part of the P-V characteristic curve has a close to linear characteristic and hence, a line passing through the origin and another point on the curve is close to a tangent enabling faster convergence.
2) Elimination of the PV curve scanning process: The PV curve scanning process is eliminated in the proposed algorithm, while the existing GFPPT algorithms require PV curve scanning at least to a certain extent [26], [27], [28], [29].
3) No power oscillations around the set point: This is an important aspect, as eliminating the steady state oscillations means that the GFPPT controller provides a constant voltage reference, v^*, after reaching the set point. However, in the conventional GFPPT algorithms [27], [29], there are no such stopping conditions. Stopping condition refers to criteria that must be satisfied in order to stop the searching process. Hence, these algorithms should constantly check if the actual power has gone more than the power reference, and if so, the actual power has to be decreased, and this happens in an oscillatory manner.
4) Need for the GMPPT convergence only when the power reference is more than the available global maximum power: The proposed IS-B GFPPT algorithm converges to the GMPP power only when the p^* is more than the available power. This is unlike the deloading-based GFPPT algorithm [27], that converges to the GMPP initially and then, reduces the power gradually to the required power reference, if the power reference is less than the GMPP power.
5) The initial parameters are chosen such that they can be easily obtained from the manufacturers' datasheet: The initialization process of the proposed IS-B GFPPT algorithm requires the values of $0.6\,v_{oc\text{-}mod}$ and $0.9\,v_{oc\text{-}str}$, which can be easily obtained from the manufacturers' datasheet, rather than performing tedious calculations as in the case of the secant-based FPPT present in the literature under uniform irradiance condition [23], [24].
6) Unlike the previous secant-based FPPT algorithm [23], the requirement of a reference curve is eliminated.
7) The error tracking and unnecessary resets during environmental change, as in the case of uniform irradiance condition [23], are also eliminated.

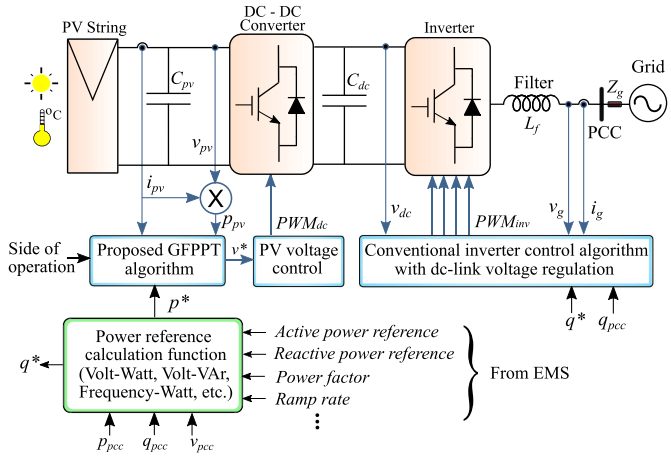

Fig. 2. Circuit diagram of the PV system employing the proposed IS-B GFPPT algorithm.

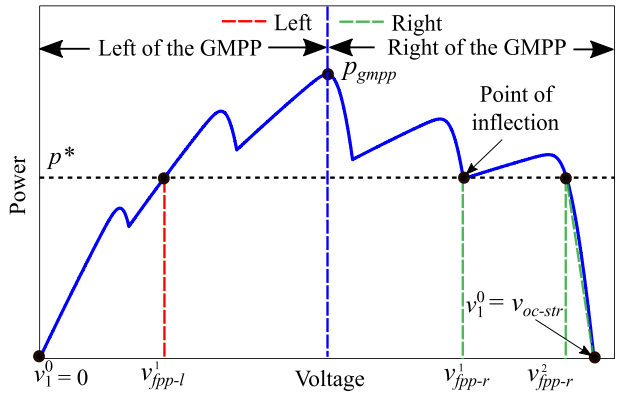

Fig. 3. Principles of the GFPPT operation in PV systems during partial shading.

The rest of this article is organized as follows. Section II explains the convergence process of the proposed IS-B GFPPT algorithm in a multimodal curve formed due to the partial shading of the solar PV modules. The detailed implementation of the proposed algorithm with its operation during different cases, such as change in power reference and environmental condition, is provided in Section III. Section IV contains the results for various test cases and discussion on the observations. Finally, Section V concludes the article.

II. Proposed Improved Secant-Based GFPPT Algorithm

This section provides the details about the employed system and the fundamental process of convergence, using the proposed IS-B GFPPT algorithm under partial shading.

A. System Description

An overview of the grid-connected PV system considered in this article is shown in Fig. 2. The proposed IS-B GFPPT algorithm is employed to generate the voltage reference for the dc–dc converter. The input commands are the reference values the controller receives. The controller should match the actual values with the received reference values. In the case of a GFPPT controller, it receives two input commands; the power reference, p^*, and the operation side. It can be seen that p^* is obtained from an external control platform, such as an EMS, that continuously monitors and optimizes the power system generation [19].

It can be seen from Fig. 3 that during partial shading of the PV modules, multiple local maximas are present. This PV characteristic is generated by using a PV string with five modules, each of them receiving a different irradiance. This P-V curve is utilized as an example in this article to illustrate the performance of the proposed IS-B GFPPT algorithm in a complex multipeak curve. The P-V curves in the article are general and the algorithm could be implemented in single or parallel string configurations.

The largest power among these maximas is the GMPP power (p_{gmpp}) and its corresponding voltage is v_{gmpp}. Further, $v_{oc\text{-}mod}$ and $v_{oc\text{-}str}$ are the open-circuit voltage of one module and the PV string, respectively, at the standard test condition (STC). As can be viewed from Fig. 3, for a given p^*, multiple voltage references are possible. They can be classified as the ones on the left-side of the GMPP ($v^i_{fpp\text{-}l}$, $i = 1,2,3,...,n_l$) and to the right of the GMPP ($v^i_{fpp\text{-}r}$, $i = 1,2,3...,n_r$). The number of possible solutions varies with respect to the shape of the curve and the value of the power reference. The proposed algorithm provides flexibility to operate at either $v^i_{fpp\text{-}l}$ or $v^i_{fpp\text{-}r}$ by selecting the voltage reference that is the closest to the initial mobile search point. Further discussions will be provided in the next subsection. Hence, the operating point can be shifted either to the left- or right-side of the GMPP according to the second control input to the GFPPT controller, as shown in Fig. 2.

The "Proposed GFPPT algorithm" block calculates the PV voltage reference, v^* according to the input commands received. This v^* corresponds to p^* received or the GMPP voltage, depending on whether p^* is smaller or larger than the GMPP power, respectively. This output v^* from the controller is fed to the PV voltage control block, which generates the pulse width modulated (PWM_{dc}) signal for the dc–dc converter. A conventional dq control with dc-link voltage regulation is employed to generate the switching pulses (PWM_{inv}) for the inverter, as shown in Fig. 2.

B. Convergence Process of the Proposed IS-B GFPPT Algorithm on a Partially Shaded PV Curve

The secant method uses numerical analysis to find the root of a nonlinear curve in a recursive manner. It shifts the operating point closer to the required solution in each iteration by estimating the intersection point of the line joining the end points of the search boundary and the power reference line. The conventional secant method is famous for not being converged in certain cases. Modifications, in terms of determining the end points in each iteration is made in the proposed IS-B FPPT algorithm in order to overcome the lack of convergence in cases where the conventional secant method fails.

To illustrate the operation of the proposed IS-B GFPPT algorithm during partial shading condition, consider a P-V characteristics as shown in Fig. 3. It can be seen that there is only one

v^* possible on the left-side of the GMPP ($v^1_{fpp\text{-}l}$) and two v^* are possible on the right-side of the GMPP ($v^1_{fpp\text{-}r}$ and $v^2_{fpp\text{-}r}$), for the given p^*. Moreover, $v^1_{fpp\text{-}r}$ lies at the point of inflection. As shown in Fig. 3, one of the initial search boundary end point, v^1_0 is chosen as 0, if the side of operation is left or $v_{oc\text{-}str}$, if the side of operation is right of the GMPP. The end point at v^0_1 is a stationary point and only the other end point, v^0_2 moves and converges to the solution.

The value of v^0_2 should be selected such that it is within the nominal operating voltage range of the dc–dc converter. There are many articles in the literature that specify the voltage range within which the GMPP voltage lies [11], [34], [35]. This voltage range is from 60% of $v_{oc\text{-}mod}$ to 90% of $v_{oc\text{-}str}$ under any environmental condition. Consequently, 60% of $v_{oc\text{-}mod}$ should lie on the left-side of the GMPP ($0.6v_{oc\text{-}mod} < v_{\text{gmpp}}$) and 90% of $v_{oc\text{-}str}$ should lie on the right-side of the GMPP ($0.9v_{oc\text{-}str} > v_{\text{gmpp}}$). Hence, v^0_2 can be selected as one of these two points depending on the operation side command. Therefore, the initial search boundary for the proposed method is given by

$$\text{left:}\begin{cases} v^0_1 = 0 \\ p^0_1 = 0 \\ v^0_2 = 0.6v_{oc\text{-}mod} \\ p^0_2 = p(v^0_2) \end{cases}, \text{ and right:}\begin{cases} v^0_1 = v_{oc\text{-}str} \\ p^0_1 = 0 \\ v^0_2 = 0.9v_{oc\text{-}str} \\ p^0_2 = p(v^0_2). \end{cases} \quad (1)$$

The voltages $0.6v_{oc\text{-}mod}$ and $0.9v_{oc\text{-}str}$ can be named as v_{min} and v_{max}, respectively, as they define the minimum and maximum limits for the GMPP voltage.

The GFPPT convergence using the proposed IS-B GFPPT algorithm is inspected in the following cases for the left-side of operation, to validate the selection of v^0_2. Hence, it is assumed that the value of v^0_2 is currently unknown, and the convergence is analysed in each case.

Case 1. $v^0_2 < v_{gmpp}$ *and* $p(v^0_2) < p^*$ Consider a case where v^0_2 is selected such that it is less than v_{gmpp} and its corresponding power, p^0_2 is less than p^*, as shown in Fig. 4(a) (i.e., $0 < p^0_2 < p^* < p_{\text{gmpp}}$). It can be seen that the voltage corresponding to the intersection point of the line joining (v^0_1, p^0_1) and (v^0_2, p^0_2) is given by v^1_2, which is sent out as the v^* for the converter to operate. Mathematically, v^* calculated from the secant method is given by

$$v^* = v^k_1 + \frac{(v^k_2 - v^k_1)(p^* - p^k_1)}{(p^k_2 - p^k_1)}, \text{ where k = 0, 1, 2,}\ldots \quad (2)$$

Hence, in the next iteration, the PV string voltage, v_{pv} and its corresponding panel power, p_{pv}, are sensed and are sent as inputs to the GFPPT controller, which updates (v_{pv}, p_{pv}) as (v^1_2, p^1_2). This process is repeated until the solution converges as given by (v^2_2, p^2_2) in the Fig. 4(a). It can also be seen that the final set point v^* is $v^1_{fpp\text{-}l}$. A similar process can be repeated for the right-side operation where *Case 1* is given by $v^0_2 > v_{\text{gmpp}}$ and $p(v^0_2) < p^*$, as shown in Fig. 4(b).

Case 2. $v^0_2 < v_{gmpp}$ *and* $p(v^0_2) > p^*$*:* In the next case, consider a scenario where the selected v^0_2 is less than v_{gmpp} such that its corresponding power, p^0_2, is more than p^*, as shown in Fig. 5(a) (i.e., $0 < p^* < p^0_2 < p_{\text{gmpp}}$). Similarly to the discussion

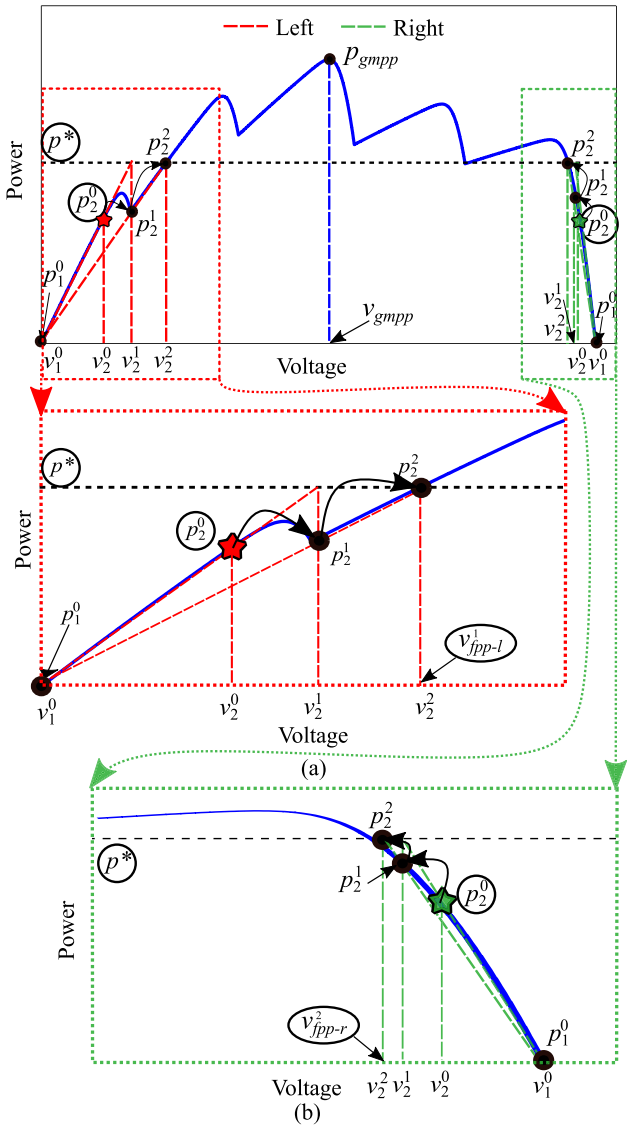

Fig. 4. *Case 1:* Convergence process while employing the proposed IS-B GFPPT algorithm when p^0_2 is less than p^*, illustrated for both sides of operation: (a) Enlarged section for the left-side of operation and (b) enlarged section for the right-side of operation.

from the previous case, the solution converges and the final set point is $v^3_2 = v^1_{fpp\text{-}l}$. A similar process can be repeated for the right-side operation where *Case 2* is given by $v^0_2 > v_{\text{gmpp}}$ and $p(v^0_2) > p^*$, as shown in Fig. 5(b).

Case 3. $v^0_2 > v_{gmpp}$*:* Finally, a third case is chosen such that the selected v^0_2 is randomly chosen to satisfy $v^0_2 > v_{\text{gmpp}}$, when the operation is selected as the left-side of the GMPP as depicted in Fig. 6. It is evident from the figure that after a few iterations, v^* becomes higher than $v_{oc\text{-}str}$ (v^3_2 will be greater than $v_{oc\text{-}str}$ in the illustrated figure). Hence, the solution does not converge if v^0_2 is initially chosen as more than v_{gmpp} during the left-side of the GMPP operation.

Hence, from the discussion, regardless of whether p^0_2 is less or more than p^*, if the condition $v^0_2 < v_{gmpp}$ is satisfied, the solution converges for the left-side of operation. Similar explanation can be extended for the right-side of operation, where

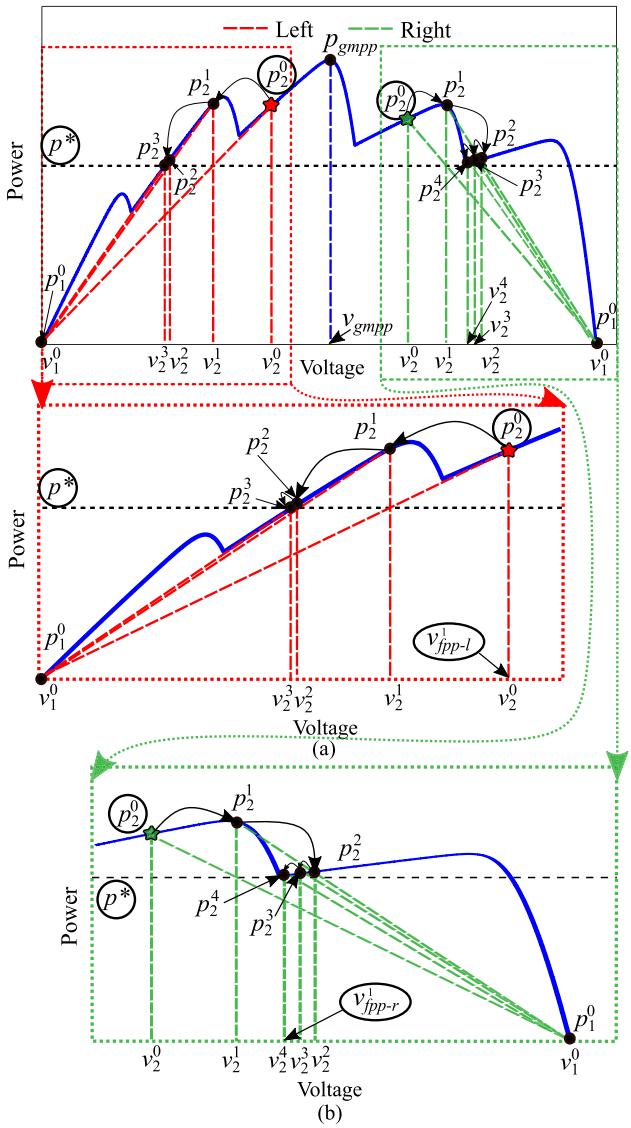

Fig. 5. *Case 2:* Convergence process while employing the proposed IS-B GFPPT algorithm when p_2^0 is more than p^*, illustrated for both sides of operation: (a) Enlarged section for the left-side of operation and (b) enlarged section for the right-side of operation.

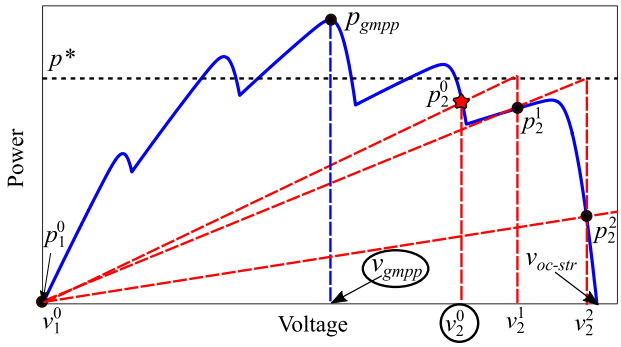

Fig. 6. *Case 3:* Improper convergence while employing the IS-B GFPPT algorithm when $v_2^0 > v_{gmpp}$ during left-side of operation.

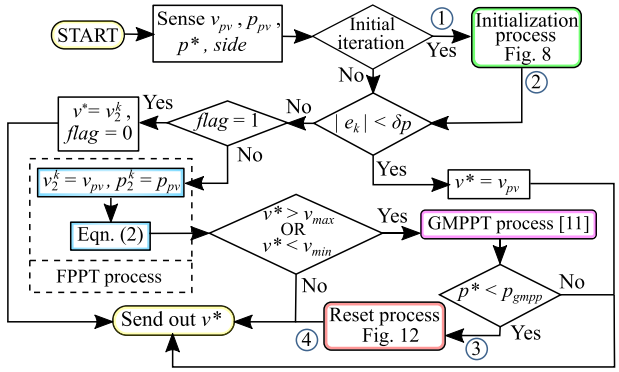

Fig. 7. Flowchart for the proposed IS-B GFPPT algorithm.

the solution will converge if $v_2^0 > v_{\text{gmpp}}$. Therefore, from the mentioned cases, it can be concluded that for the proposed IS-B GFPPT algorithm to achieve convergence, the following criteria should be satisfied:

$$\text{For convergence:} \begin{cases} 0 < v_2^0 < v_{\text{gmpp}}, & \text{if left-side} \\ v_{gmpp} < v_2^0 < v_{oc\text{-}str}, & \text{if right-side.} \end{cases} \tag{3}$$

It is discussed that $0.6\,v_{oc\text{-}mod}$ will lie on the left-side of the GMPP ($0{<}0.6v_{oc\text{-}mod} < v_{\text{gmpp}}$) and $0.9\,v_{oc\text{-}str}$ will lie on the right-side of the GMPP ($v_{\text{gmpp}} < 0.9v_{oc\text{-}str} < v_{oc\text{-}str}$). Hence, these points satisfy (3), thereby justifying the selection of the mentioned initial search boundary in (1). It is noted that the convergence issue, discussed in *Case 3* (Fig. 6), is eliminated by this selection. This is because $0.6v_{oc\text{-}mod}$ will be never more than v_{gmpp}, and *Case 3* will not occur. Hence, by selection of these initial search points, convergence can be guaranteed in the proposed IS-B GFPPT algorithm.

During the right-side of operation, it can be viewed from Figs. 4(b) and 5(b), respectively, that the final set point v^* is $v_{fpp\text{-}r}^2$ in the first case and $v_{fpp\text{-}r}^1$ in the second case. Hence, it can be concluded that the final set point v^* is the $v_{fpp\text{-}r}^i$ closest to the initial end point, v_2^0. Moreover, $v_{fpp\text{-}r}^1$ lies exactly at the point of inflection where the proposed algorithm tracks without any difficulty.

III. Implementation of the Proposed Improved Secant-Based GFPPT Algorithm

The flowchart for the proposed IS-B GFPPT algorithm during partial shading of the PV system is depicted in Fig. 7. As discussed in Section II-A, the GFPPT control algorithm receives the power reference, p^*, side of operation, sensed PV panel voltage, v_{pv}, and its corresponding power, p_{pv}, as the inputs. Firstly, the algorithm needs to be initialized. As discussed in Section II-B, the initial search boundary is fixed as depicted in Fig. 8.

It can be seen that the power at v_2^0 is required to initialize the search boundary. Hence, a variable, $flag$, is set as 1 to output the voltage reference, v^* as v_2^0 at the first iteration and the measured p_{pv} obtained is set as $p(v_2^0)$. During the subsequent iterations,

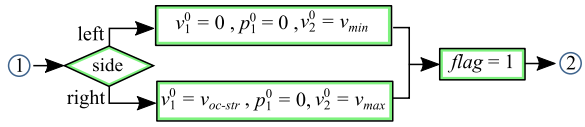

Fig. 8. Initialization process.

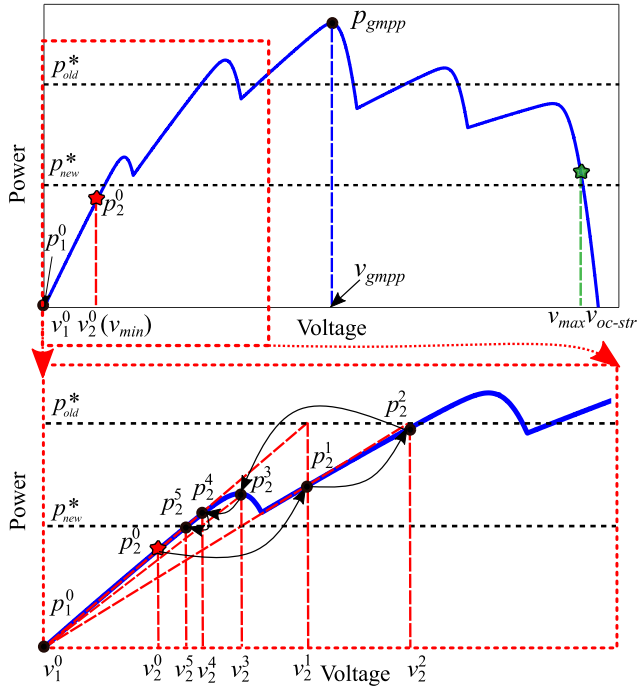

Fig. 9. *Case A:* Convergence process of the proposed IS-B GFPPT algorithm when p^* changes.

$flag$ is reset to 0 and the main GFPPT process takes place. The convergence process of the proposed IS-B GFPPT algorithm was discussed in Section II. The convergence of the solution is realized when the error, e_k becomes less than a set tolerance, δ_p, as follows:

$$|e_k| = |p^* - p_{\text{pv}}| < \delta_p. \tag{4}$$

The value of δ_p can be regarded as 1% of the nominal power value at STC under uniform irradiance condition. If $|e_k| < \delta_p$, v_{pv} is given out as v^*, else the GFPPT process takes place as shown in Fig. 7.

It is important to inspect different cases to ensure that the controller does not diverge from the solution. Such cases are discussed as follows considering left-side of operation (similar arguments can be extended for operation on the right-side).

Case A: Change in Power Reference

p^* command obtained from the EMS changes frequently according to the power system requirements. Hence, the performance of the proposed algorithm should be examined during such a condition, as depicted in Fig. 9. The initial p^* is denoted as p^*_{old} and it can be seen that in two iterations, the solution is converged. When the power reference suddenly changes to p^*_{new},

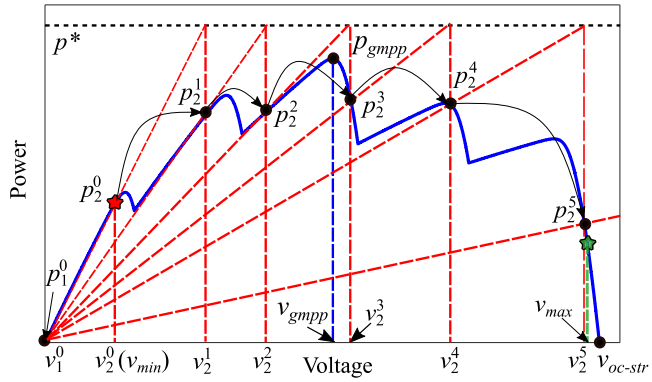

Fig. 10. *Case B:* Convergence process of the proposed IS-B GFPPT algorithm when p^* is more than p_{gmpp}.

as long as $v^* < v_{\text{gmpp}}$ for left-side of operation, the proposed IS-B GFPPT algorithm readily converges to the new p^*. It is seen from Fig. 9 that with three more iterations, p_2^5 converges to p^*_{new}.

Case B: $p^* \geq p_{gmpp}$

For the previous case, it was assumed that p^* is less than p_{gmpp}. However, if the amount of PV power is insufficient to meet the demand, the GFPPT needs to converge to the GMPP. Such a scenario is depicted in Fig. 10. Considering left-side of operation, v_1^0 and v_2^0 are set as 0 and v_{min}, respectively. Applying the proposed IS-B GFPPT algorithm, it can be seen that after a few iterations, v_2^5 becomes more than v_{max}. Since v_{max} lies on the right-side of the GMPP and the command provided is left-side operation, $v^* > v_{\text{max}}$, implying that the power reference cannot be attained, i.e., $p^* > p_{\text{gmpp}}$. In this situation, the controller should shift the operating mode from the GFPPT to the GMPPT in order to give out the maximum possible power. This can be achieved by employing any of the GMPPT algorithms presented in the literature for partial shaded PV system [8], [9], [10], [11], [12], [13], [14], [15], [16], [36]. In this article, the SSJ-GMPPT algorithm [11] is used for tracking the GMPP with high accuracy and speed without requiring any additional circuits or sensors.

This constitutes the next step in the implementation of the proposed method, as seen in Fig. 7. There is a check on whether v^* is between v_{min} and v_{max} to ensure if $0 < p^* < p_{\text{gmpp}}$, else the GMPPT process is implemented.

Case C: Change in Environmental Conditions

In this case, a change in the environment, such as a cloud passing that creates a change in partial shading conditions, is to be inspected. Fig. 11(a) illustrates a condition when the power at the GMPP of the old P-V characteristics curve, $p^{\text{old}}_{\text{gmpp}}$ is more than the GMPP power of the new P-V curve. As seen, the convergence takes place in the old curve, and then the shift to the new curve occurs. Subsequently, p_2^1 on the old curve is reflected as p_2^2 on the new curve for the same voltage reference. Then, the proposed GFPPT process continues and the solution is converged within three iterations in the new curve.

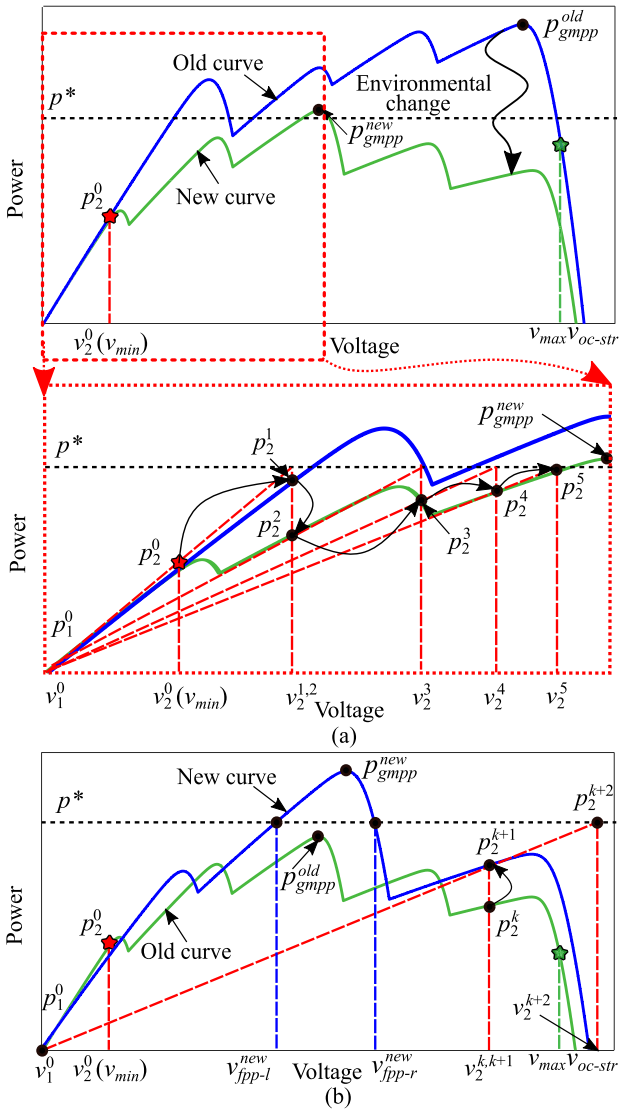

Fig. 11. *Case C:* Convergence process of the proposed IS-B GFPPT algorithm during environmental change: (a) Proper convergence and (b) improper convergence.

However, in the next scenario, $p^{\text{old}}_{\text{gmpp}} < p^{\text{new}}_{\text{gmpp}}$ as depicted in Fig. 11(b), the GFPPT controller makes the wrong decision and the solution does not converge. Consider an ongoing operation on the left-side in the old curve such that the current operating point is (v_2^k, p_2^k). This point is achievable as $p^* \geq p^{\text{old}}_{\text{gmpp}}$ and hence, v_2^k has gone beyond v_{gmpp}. If there is a change in the curve to a new one, as shown in Fig. 11(b), p_2^k will be reflected as p_2^{k+1} in the new curve. The GFPPT process continues and v_2^{k+2} becomes more than v_{max}. Accordingly, the GMPPT process will be initiated. However, this is incorrect as it is clearly visible in Fig. 11(b) that two voltage references are possible ($v^{\text{new}}_{fpp\text{-}l}$ and $v^{\text{new}}_{fpp\text{-}r}$) for the given p^* and the solution should have converged to $v^{\text{new}}_{fpp\text{-}l}$.

To overcome this issue, there is a check on whether p^* is less than p_{gmpp}. If so, the stated misjudgement has occurred, and the algorithm needs to be reset to its initial boundary conditions. The reset process is as depicted in Fig. 12. However, if $p^* > p_{\text{gmpp}}$, the GMPPT process is correct and the control point stays at p_{gmpp} and v_{gmpp} is sent out as v^* until any change occurs.

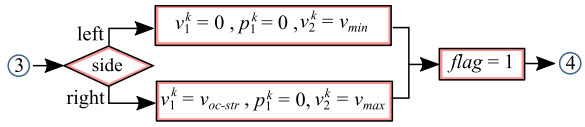

Fig. 12. Reset process.

TABLE I
EXPERIMENTAL SETUP PARAMETERS

Parameter	Value
PV string maximum power, p_{gmpp}	950 W
PV string voltage at the GMPP, v_{gmpp}	145 V
PV string open circuit voltage, $v_{oc\text{-}str}$	173 V
PV side capacitance, C_{pv}	20 μF
Boost converter inductance, L	2.36 mH
DC link voltage, V_{dc}	175 V
Switching frequency, f_s	50 kHz

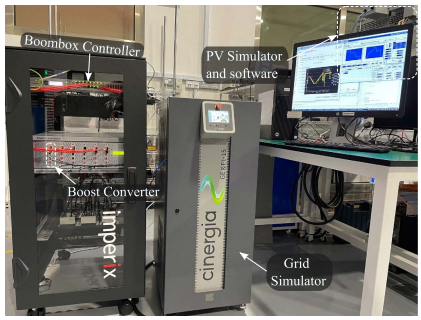

Fig. 13. Experimental setup.

IV. RESULTS AND DISCUSSION

To demonstrate the efficacy of the proposed IS-B GFPPT algorithm, experimental evaluation is performed on a PV system whose parameters are listed in Table I. A photo of the set-up is shown in Fig. 13. The PV panel is simulated using a Chroma 62000H-S solar array simulator. The GFPPT algorithm is implemented in an Imperix B-Box RCP digital controller.

In the following experiments, three series-connected PV modules form a PV string. The partial shading phenomenon is created by changing the irradiance level of the modules as shown in Fig. 14. The test cases for change in p^* and partial shading conditions are considered to assess the proposed IS-B GFPPT algorithm for the left-side of the GMPP operation.

A. Step Changes in Power Reference

Step changes in p^* are given to the the proposed IS-B GFPPT algorithm to observe its power tracking capability. Curve C from Fig. 14 is opted for this test case.

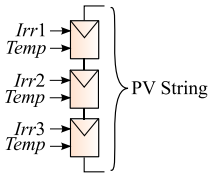

Temp = 25°C

PV Curve	Irradiance (W/m²)			GMPP Power (W)
	*Irr*1	*Irr*2	*Irr*3	P_{gmpp}
Curve A	1000	1000	1000	950
Curve B	1000	800	650	692
Curve C	1000	300	700	484

Fig. 14. Details of the PV curves used for the experimental test cases.

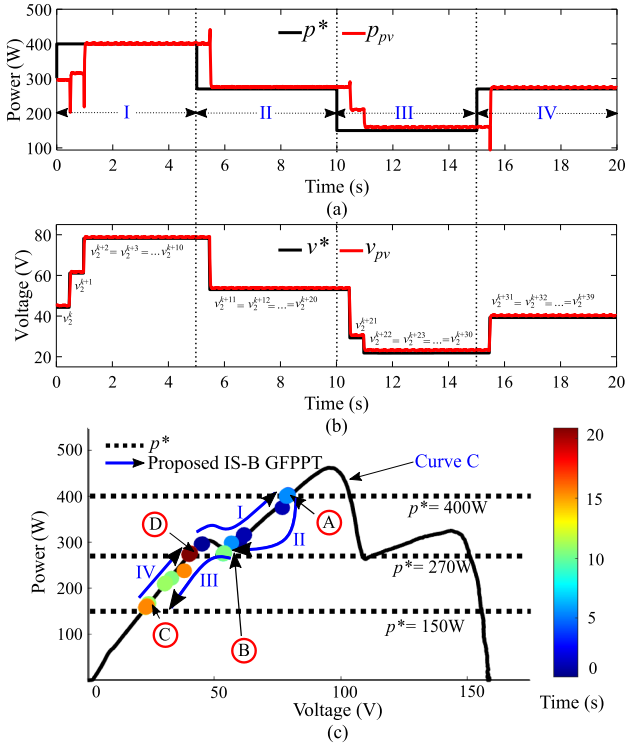

Fig. 15. Experimental results using the proposed IS-B GFPPT algorithm for step changes in power reference: (a) PV power and power reference, (b) PV voltage and (c) P-V operation point.

The results are shown in Fig. 15. Initially the PV string is operated at $p^* = 300$ W. At $t = 0$ s, p^* is increased to 400 W, whose steady state set point is given by point A in Fig. 15(c). Consider that the algorithm is at the kth iteration, when the p^* was changed from 300 W to 400 W. The time step, T_{step} of the GFPPT controller is 0.5 s. Hence, a new iteration starts after each 0.5 s, where the controller updates the v^*. It can be seen from Fig. 15(a) that p_{pv} reaches p^* in three iterations, with a corresponding voltage of v_2^{k+2} as depicted in Fig. 15(b). Hence, until further changes in p^*, the v^* stays the same. At $t = 5$ s, p^* is decreased to 270 W, given by point B. Therefore, until v_2^{k+10}, the PV voltage value will remain as v_2^{k+2}. It can be seen that point B is the point of inflection on Curve C and the proposed IS-B GFPPT algorithm is able to track the power reference at this point. This tracking is done without extracting any additional data as in the case of [26]. At $t = 10$ s, p^* is decreased further to 150 W, given by point C. Finally, at $t = 15$ s, p^* is increased back to 270 W. It can be seen that the settling point in this case is at point D, rather than point B seen previously. This is due to the fact that the proposed IS-B GFPPT algorithm converges to the nearest solution.

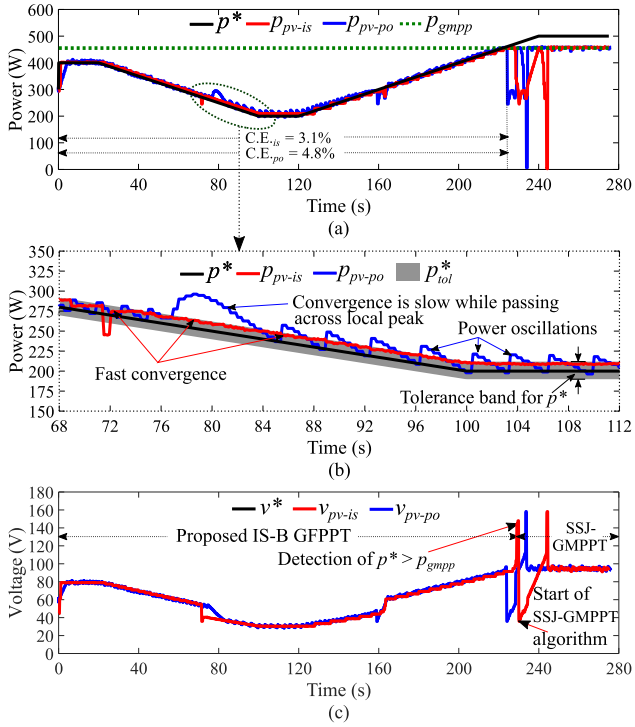

Fig. 16. Experimental results. Comparison of the proposed IS-B GFPPT algorithm and the P&O-based GFPPT algorithm [29] for linear change in power reference: (a) PV power and power reference, (b) enlarged section showing PV power with the power reference tolerance band (p^*_{tol}), and (c) PV voltage. Subscript: "*pv-is*" - proposed IS-B GFPPT algorithm, "*pv-po*" - P&O-based GFPPT algorithm [29].

It can be seen from this figure that the proposed IS-B GFPPT algorithm is able to track p^* without any reset even when p^* changes. Moreover, there are no power oscillations around the set point.

B. Linear Change in Power Reference

The power reference command received might vary in a linear fashion and hence, a linear change in p^* is provided for the proposed IS-B GFPPT algorithm as shown in Fig. 16(a). Curve C from Fig. 14 is opted for this test case. The proposed IS-B GFPPT algorithm is compared with the P&O-based GFPPT algorithm [29] through experimental analysis for this test case. As the P&O-based algorithms converge efficiently whenever a linear change is present (because of the constant voltage step), this case is selected for comparison to represent the efficacy of the proposed algorithm.

Initially the PV string is operated at $p^* = 300$ W. At $t = 0$ s, p^* is increased to 400 W. Then, p^* is decreased linearly from $p^* = 400$ W to $p^* = 200$ W and kept at 200 W till $t = 120$ s. Then, it is increased linearly from $p^* = 200$ W to $p^* = 500$ W and kept at 500 W thereafter.

The p_{gmpp} of Curve C is at 484 W. It can be seen from Fig. 16(a) that both algorithms track the p^* if it is less than 484 W. (the subscript "pv-is" refer to the PV parameters corresponding

to the proposed IS-B GFPPT algorithm and "pv-po" refer to the PV parameters corresponding to the P&O-based GFPPT algorithm). However, as seen from the enlarged section near a local peak, as shown in Fig. 16(b), the P&O-based GFPPT algorithm cannot track the p^* in the given time but the proposed IS-B GFPPT is able to achieve it without any difficulty. Moreover, it can be seen from Fig. 16(b) that power oscillations are present around the set point while employing the P&O-based GFPPT algorithm. However, the proposed IS-B GFPPT algorithm does not create any power oscillations around the set point. The difference between p^* and $p_{pv\text{-}is}$ is about 10 W and is due to the tolerance, δ_p (shown in Fig. 16(b) as a p^* tolerance band, p^*_{tol}). The constant voltage step (v_{step}) for the P&O-based GFPPT algorithm is chosen as 2 V (1 % of v_{oc} at STC). Larger values of the v_{step} can result in faster convergence, however, the power oscillations will be more.

After around 230 s, p^* increases beyond 484 W (p_{gmpp}). Hence, it can be seen from Fig. 16(c) that v^* goes beyond v_{max} in the proposed IS-B GFPPT algorithm. This is used to detect the scenario when p^* exceeds the maximum available power. Therefore, the GFPPT algorithms shift to the SSJ-GMPPT algorithm as depicted in Fig. 16(c). After detecting this condition, v^* resets to v_{min} and the SSJ-GMPPT algorithm starts its operation. The SSJ GMPPT algorithm scans the curve and stores the values of local peaks until the global peak is encountered. After judging the global peak, the subsequent local curves are skipped until v^* becomes more than v_{max} (which is seen as the second spike after 240 s). Then, the SSJ algorithm goes back to the detected global peak and settles there. The P&O GFPPT method also experiences a similar GMPP convergence because it uses the SSJ GMPPT algorithm as well.

It is to be noted that the GMPPT process occurs only when $p^* > p_{\text{gmpp}}$ in the proposed IS-B FPPT algorithm. This substantially reduces the algorithm convergence time compared to [27], [28] where the GMPP convergence occurs each time, irrespective of whether $p^* > p_{\text{gmpp}}$ or $p^* < p_{\text{gmpp}}$.

To evaluate the performance of the GFPPT algorithm mathematically, the cumulative error (C.E.) is calculated in each of the test cases, given by

$$\text{C.E.} = \frac{\int_{t_0}^{t_n} |p^* - p_{pv}|\, dt}{\int_{t_0}^{t_n} |p^*|\, dt} \times 100. \tag{5}$$

The C.E. calculated for the proposed IS-B GFPPT algorithm is 3.1 % and it is 4.8 % for the P&O-based GFPPT algorithm. The mentioned comparisons are summarized and listed in Table II.

TABLE II
PERFORMANCE COMPARISON BETWEEN THE P&O-BASED AND THE PROPOSED IS-B GFPPT ALGORITHM

Feature	P&O-based GFPPT [29]	Proposed IS-B GFPPT
v^* **generation**	Fixed voltage step	From secant formula
Convergence	Guaranteed but slow	Guaranteed and fast
C.E. (for variable p^* test case)	4.8%	3.1%
Power oscillations around the set point	Present	Absent

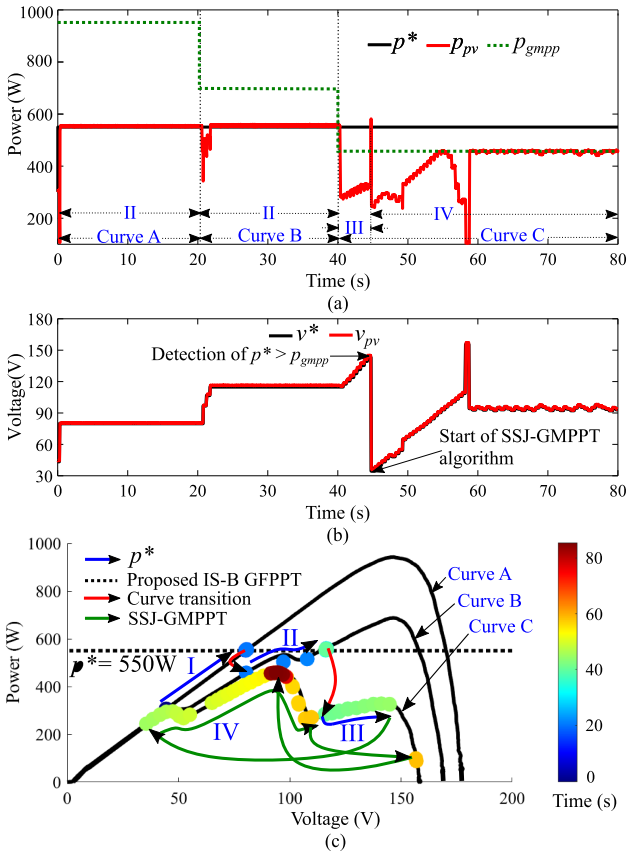

Fig. 17. Experimental results using the proposed IS-B GFPPT algorithm for change in partial shading condition: (a) PV power and power reference, (b) PV voltage, and (c) P-V operation point.

C. Performance Under Partial Shading Conditions

In this case, a partial shading change is considered, keeping p^* constant at 550 W as shown in Fig. 17.

Curves A, B, and C from Fig. 14 are opted for this case. From $t = 0$ s to $t = 20$ s, Curve A is considered. Since p_{gmpp} of Curve A is more than p^*, the power is tracked by the proposed IS-B GFPPT algorithm. Next, Curve B is considered from $t = 20$ s to $t = 40$ s. Even though the partial shading conditions are changed, still p_{gmpp} of Curve B is more than p^*, and hence, the power is being tracked in this case also. Finally, at $t = 40$ s, a shift to Curve C occurs. In this case, p_{gmpp} of Curve C is less than p^*, and hence, the proposed IS-B GFPPT algorithm detects this condition when v^* becomes greater than v_{max}. Subsequently, the SSJ-GMPPT algorithm starts its operation from v_{min}, to converge to the GMPP power of Curve C. When the controller is operating in the GMPPT mode and if a change in partial shading condition occurs while in the convergence process, a strategy as employed in [21] is opted to detect such changes. If the GFPPT controller is working at a time step (T_{step}), then the instantaneous PV voltage can be denoted as $v_{\text{pv}}(t)$, where $t = k * T_{\text{step}}$. The PV power at both $v_{\text{pv}}(t)$ and $v_{\text{pv}}(t - 0.5T_{\text{step}})$ are recorded and their difference is used to determine if there are any changes in the partial shading condition.

TABLE III
COMPARISON BETWEEN DIFFERENT GFPPT ALGORITHMS

GFPPT algorithms	PV curve scanning	Requirement to find LMPP/ point of inflection	GMPP convergence	Algorithm complexity	Power oscillations around the set point
Curve fitting [26]	Required	Required	Only when $p^* > p_{gmpp}$	Medium	Not present
Deloading [27]	From p_{gmpp} power to p^*	Not required	For every p^* change	Low	Present
HC&PSO [28]	From LMPP power to p^*	Required	Only when $p^* > p_{gmpp}$	High	Not present
P&O [29]	From old p^* to new p^*	Not required	Only when $p^* > p_{gmpp}$	Low	Present
Proposed IS-B GFPPT	Not required	Not required	Only when $p^* > p_{gmpp}$	Low	Not present

D. Discussion

The performance of the proposed IS-B GFPPT algorithm is compared with the GFPPT algorithms presented in the literature [26], [27], [28], [29], as listed in Table III. It can be seen that the requirement of PV curve scanning is eliminated in the proposed IS-B GFPPT algorithm, while the other GFPPT algorithms require PV curve scanning to an extent. Unlike [26] and [28], there is also no requirement to find the LMPPs or the point of inflection for the operation of the proposed algorithm. The initial set points can also be obtained easily from the manufacturers' datasheet. Moreover, the GMPP convergence is only required when $p^* > p_{\text{gmpp}}$ as seen in the test cases IV B and C. Since the proposed algorithm uses a simple expression to calculate v^* (2) with the aid of simple decision-making statements to converge to the solution, its complexity is also very low. Finally, the power oscillations around the set point are eliminated in the proposed IS-B GFPPT algorithm.

V. CONCLUSION

A fast GFPPT algorithm based on an improved secant method that works effectively during partial shading conditions of a PV string has been proposed in this article. This algorithm guarantees convergence to the power reference in an efficient manner, by avoiding unnecessary resets during changes in power reference or environmental conditions. Moreover, the proposed algorithm can track intricate points such as the power reference at the point of inflection without any difficulty. The performance of the proposed IS-B GFPPT algorithm has been evaluated experimentally under various test cases and is compared against a recent P&O-based GFPPT algorithm. Results showcase effective operation of the proposed IS-B GFPPT algorithm with minimal error.

REFERENCES

[1] D. Gielen, F. Boshell, D. Saygin, M. D. Bazilian, N. Wagner, and R. Gorini, "The role of renewable energy in the global energy transformation," *Energy Strategy Rev.*, vol. 24, pp. 38–50, Apr. 2019.

[2] E. Kabir, P. Kumar, S. Kumar, A. A. Adelodun, and K.-H. Kim, "Solar energy: Potential and future prospects," *Renew. Sustain. Energy Rev.*, vol. 82, pp. 894–900, Feb. 2018.

[3] R. B. Bollipo, S. Mikkili, and P. K. Bonthagorla, "Critical review on PV MPPT techniques: Classical, intelligent and optimisation," *IET Renew. Power Gener.*, vol. 14, no. 9, pp. 1433–1452, Jun. 2020.

[4] A. K. Podder, N. K. Roy, and H. R. Pota, "MPPT methods for solar PV systems: A critical review based on tracking nature," *IET Renew. Power Gener.*, vol. 13, no. 10, pp. 1615–1632, Jul. 2019.

[5] S. K. Kollimalla and M. K. Mishra, "Variable perturbation size adaptive p&o MPPT algorithm for sudden changes in irradiance," *IEEE Trans. Sustain. Energy*, vol. 5, no. 3, pp. 718–728, Jul. 2014.

[6] S. Mohanty, B. Subudhi, and P. K. Ray, "A grey wolf-assisted perturb & observe MPPT algorithm for a PV system," *IEEE Trans. Energy Convers.*, vol. 32, no. 1, pp. 340–347, Mar. 2017.

[7] N. E. Zakzouk, M. A. Elsaharty, A. K. Abdelsalam, A. A. Helal, and B. W. Williams, "Improved performance low-cost incremental conductance PV MPPT technique," *IET Renew. Power Gener.*, vol. 10, no. 4, pp. 561–574, Apr. 2016.

[8] M. Dhimish, "Assessing MPPT techniques on hot-spotted and partially shaded photovoltaic modules: Comprehensive review based on experimental data," *IEEE Trans. Electron. Devices*, vol. 66, no. 3, pp. 1132–1144, Mar. 2019.

[9] J. Ahmed and Z. Salam, "An enhanced adaptive p&o MPPT for fast and efficient tracking under varying environmental conditions," *IEEE Trans. Sustain. Energy*, vol. 9, no. 3, pp. 1487–1496, Jul. 2018.

[10] A. Ramyar, H. Iman-Eini, and S. Farhangi, "Global maximum power point tracking method for photovoltaic arrays under partial shading conditions," *IEEE trans. Ind. Electron.*, vol. 64, no. 4, pp. 2855–2864, Apr. 2017.

[11] Y. Wang, Y. Li, and X. Ruan, "High-accuracy and fast-speed MPPT methods for PV string under partially shaded conditions," *IEEE Trans. Ind. Electron.*, vol. 63, no. 1, pp. 235–245, Jan. 2016.

[12] H. Rezk, M. Aly, M. Al-Dhaifallah, and M. Shoyama, "Design and hardware implementation of new adaptive fuzzy logic-based MPPT control method for photovoltaic applications," *IEEE Access*, vol. 7, pp. 106427–106438, 2019.

[13] N. Kumar, B. Singh, and B. K. Panigrahi, "PNKLMF-based neural network control and learning-based HC MPPT technique for multiobjective grid integrated solar PV based distributed generating system," *IEEE Trans. Ind. Informat.*, vol. 15, no. 6, pp. 3732–3742, Jun. 2019.

[14] H. Li, D. Yang, W. Su, J. Lü, and X. Yu, "An overall distribution particle swarm optimization MPPT algorithm for photovoltaic system under partial shading," *IEEE Trans. Ind. Electron.*, vol. 66, no. 1, pp. 265–275, Jan. 2019.

[15] R. B. Koad, A. F. Zobaa, and A. El-Shahat, "A novel MPPT algorithm based on particle swarm optimization for photovoltaic systems," *IEEE Trans. Sustain. Energy*, vol. 8, no. 2, pp. 468–476, Apr. 2017.

[16] S. Mohanty, B. Subudhi, and P. K. Ray, "A new MPPT design using grey wolf optimization technique for photovoltaic system under partial shading conditions," *IEEE Trans. Sustain. Energy*, vol. 7, no. 1, pp. 181–188, Jan. 2016.

[17] H. D. Tafti et al., "Extended functionalities of photovoltaic systems with flexible power point tracking: Recent advances," *IEEE Trans. Power Electron.*, vol. 35, no. 9, pp. 9342–9356, Sep. 2020.

[18] A. Kumaresan, H. D. Tafti, G. G. Farivar, N. B. Y. Gorla, N. Beniwal, and J. Pou, "Performance comparison of flexible power point tracking algorithms on normal and degraded photovolatic modules," in *Proc. IEEE 7th Southern Power Electron. Conf.*, 2022, pp. 1–6.

[19] F. Yang, X. Feng, and Z. Li, "Advanced microgrid energy management system for future sustainable and resilient power grid," *IEEE Trans. Ind. Appl.*, vol. 55, no. 6, pp. 7251–7260, Nov./Dec. 2019.

[20] H. D. Tafti, C. D. Townsend, G. Konstantinou, and J. Pou, "A multimode flexible power point tracking algorithm for photovoltaic power plants," *IEEE Trans. Power Electron.*, vol. 34, no. 6, pp. 5038–5042, Jun. 2019.

[21] H. D. Tafti, A. Sangwongwanich, Y. Yang, J. Pou, G. Konstantinou, and F. Blaabjerg, "An adaptive control scheme for flexible power point tracking in photovoltaic systems," *IEEE Trans. Power Electron.*, vol. 34, no. 6, pp. 5451–5463, Jun. 2019.

[22] R. Gomez-Merchan et al., "Binary search based flexible power point tracking algorithm for photovoltaic systems," *IEEE Trans. Ind. Electron.*, vol. 68, no. 7, pp. 5909–5920, Jul. 2021.

[23] A. Kumaresan, H. D. Tafti, N. K. Kandasamy, G. G. Farivar, J. Pou, and T. Subbaiyan, "Flexible power point tracking for solar photovoltaic systems using secant method," *IEEE Trans. Power Electron.*, vol. 36, no. 8, pp. 9419–9429, Aug. 2021.
[24] A. Kumaresan, H. D. Tafti, G. G. Farivar, K. N. Kumar, and J. Pou, "Secant-based flexible power point tracking algorithm for degraded photovoltaic systems," in *Proc. IEEE Energy Convers. Congr. Expo.*, 2021, pp. 925–930.
[25] A. Kumaresan, H. D. Tafti, G. G. Farivar, N. B. Y. Gorla, N. Beniwal, and J. Pou, "Flexible power point tracking algorithm using the newton's method," in *Proc. IEEE 47th Annu. Conf. Ind. Electron. Soc.*, 2021, pp. 1–6.
[26] E. I. Batzelis, S. A. Papathanassiou, and B. C. Pal, "PV system control to provide active power reserves under partial shading conditions," *IEEE Trans. Power Electron.*, vol. 33, no. 11, pp. 9163–9175, Nov. 2018.
[27] P. Verma, T. Kaur, and R. Kaur, "Power control strategy of PV system for active power reserve under partial shading conditions," *Int. J. Elect. Power Energy Syst.*, vol. 130, Sep. 2021, Art. no. 106951.
[28] Z. Xie and Z. Wu, "A flexible power point tracking algorithm for photovoltaic system under partial shading condition," *Sustain. Energy Technol. Assessments*, vol. 49, Feb. 2022, Art. no. 101747.
[29] H. D. Tafti, Q. Wang, C. D. Townsend, J. Pou, and G. Konstantinou, "Global flexible power point tracking in photovoltaic systems under partial shading conditions," *IEEE Trans. Power Electron.*, vol. 37, no. 9, pp. 11332–11341, Sep. 2022.
[30] J. Ehiwario and S. Aghamie, "Comparative study of bisection, newton-raphson and secant methods of root-finding problems," *IOSR J. Eng.*, vol. 4, no. 4, pp. 1–7, Apr. 2014.
[31] J. M. Papakonstantinou and R. A. Tapia, "Origin and evolution of the secant method in one dimension," *Amer. Math. Monthly*, vol. 120, no. 6, pp. 500–517, Jun.-Jul. 2013.
[32] R. A. Adams and C. Essex, *Calculus: A. Complete Course*, vol. 4. Addison-Wesley Boston, Jan. 1999.
[33] P. Díez, "A note on the convergence of the secant method for simple and multiple roots," *Appl. Math. Lett.*, vol. 16, no. 8, pp. 1211–1215, Nov. 2003.
[34] A. M. Furtado, F. Bradaschia, M. C. Cavalcanti, and L. R. Limongi, "A reduced voltage range global maximum power point tracking algorithm for photovoltaic systems under partial shading conditions," *IEEE Trans. Ind. Electron.*, vol. 65, no. 4, pp. 3252–3262, Apr. 2018.
[35] M. Kermadi, Z. Salam, J. Ahmed, and E. M. Berkouk, "An effective hybrid maximum power point tracker of photovoltaic arrays for complex partial shading conditions," *IEEE Trans. Ind. Electron.*, vol. 66, no. 9, pp. 6990–7000, Sep. 2019.
[36] A. Kumaresan, G. G. Farivar, H. D. Tafti, N. Beniwal, N. B. Y. Gorla, and J. Pou, "Global maximum power point tracking for photovoltaic systems using hybrid secant and binary search algorithms," in *Proc. IEEE Energy Convers. Congr. Expo.*, 2022, pp. 1–6.

Anusha Kumaresan (Student Member, IEEE) received the B.E. degree in electrical and electronics engineering from Anna University, Chennai, India, in 2018, and the M.Tech. degree in power electronics from the National Institute of Technology Puducherry, Karaikal, UT of Puducherry, India, in 2020. She is currently working toward the Ph.D. degree in power electronics with the Energy Research Institute, Interdisciplinary Graduate Programme, Nanyang Technological University, Singapore.

From August 2019 to February 2020, she was a Visiting Student with the Singapore University of Technology and Design, Singapore. She is also on a research exchange to the SENSE - Chair for Sustainable Electric Networks and Sources of Energy with Technische Universität Berlin, Berlin, Germany. Her research interests include renewable energy systems, electrical machines, and drives.

Hossein Dehghani Tafti (Senior Member, IEEE) received the B.Sc. and M.Sc. degrees in electrical engineering and power system engineering from the Amirkabir University of Technology, Tehran, Iran, in 2009 and 2011, respectively, and the Ph.D. degree in electrical engineering from Nanyang Technological University, Singapore, in 2018.

From January 2018 to April 2020, he was a Research Fellow with Nanyang Technological University, where he was working on the control of photovoltaic systems for grid support. From May 2020 to May 2021, he was a Senior Research Associate with the University of New South Wales, Sydney, Australia, where he worked on modeling and testing of commercial photovoltaic inverters. He is currently a Research Fellow with the Department of Electrical, Electronic and Computer Engineering, University of Western Australia, Perth, WA, Australia. His research interests include the grid-integration of renewable energy sources, in particular, photovoltaics and energy storage and design and control of multilevel power converters.

Neha Beniwal (Member, IEEE) received the B.Tech. degree in electrical engineering from the National Institute of Technology, Kurukshetra, India, in 2014, the M.Tech. degree in power electronics, electrical machines and drives (PEEMD) from the Indian Institute of Technology, Delhi, India, in 2017, and the Ph.D. degree in power electronics from the Interdisciplinary Graduate School, Nanyang Technological University (NTU), Singapore, in 2021.

She is currently a Research Engineer with GE Global Research, NY, USA. Prior to this, she was working as a Research Fellow with the Energy Research Institute, NTU (ERI@N), Singapore. Her research interests include modulation and control of power converters for renewable energy integration, aerospace and energy storage systems.

Dr. Beniwal was the recipient of the Commendation for Doctorate Research Excellence Award for her outstanding Ph.D. research work by the School of EEE, NTU, Singapore, the POSOCO Power System Award, awarded by Power System Operation Corporation Ltd. (POSOCO) in association with Foundation for Innovation and Technology Transfer in 2018 for her master's research work, and the Prof. A.K. Sinha Cash Prize and IEEE-PEDES'96 Award at the Annual Convocation of the Indian Institute of Technology Delhi, New Delhi, India, in 2017.

Naga Brahmendra Yadav Gorla (Senior Member, IEEE) received the M.S. degree (by research) from the Indian Institute of Technology Madras, Chennai, India, and the Ph.D. degree in electrical engineering from the National University of Singapore, Singapore, in 2013 and 2019, respectively.

From October 2013 to December 2015, he was with the Department of Electrical and Electronics, Singapore Polytechnic, Singapore, as a Research Engineer. From April 2019 to July 2020, he was a Research Fellow with Sembcorp-NUS Corporate Laboratory, National University of Singapore. From July 2020 to January 2023, he was a Research Fellow with Energy Research Institute, Nanyang Technological University (ERI@N), Singapore. He is currently an Assistant Professor with the Indian Institute of Technology Palakkad, Kerala, India. His research interests include electromagnetic interference issues in wide bandgap-based power converters, fault diagnosis and fault tolerant control of modular power converters, and renewable energy systems.

Glen G. Farivar (Senior Member, IEEE) received the B.Sc. degree in electrical engineering from the Nooshirvani Institute of Technology, Babol, Iran, in 2008, the M.Sc degree in power electronics from the University of Tehran, Tehran, Iran in 2011, and the Ph.D. degree in electrical engineering from the University of NSW Australia, Sydney, Australia, in 2016.

He is currently working as a Lecturer with the University of Melbourne, Melbourne, Australia. He is a cofounder of SciLeap, which aims to promote research integrity, accessibility, and openness. His research interests include renewable energy systems, high power converters, energy storage, FACTS, and electric vehicles.

Josep Pou (Fellow, IEEE) received the B.S., M.S., and Ph.D. degrees in electrical engineering from the Technical University of Catalonia (UPC)-Barcelona Tech, Barcelona, Spain, in 1989, 1996, and 2002, respectively.

In 1990, he joined the faculty of UPC as an Assistant Professor, where he became an Associate Professor in 1993. From February 2013 to August 2016, he was a Professor with the University of New South Wales (UNSW), Sydney, Australia. He is currently a Professor with the Nanyang Technological University (NTU), Singapore, where he is Cluster Director of Power Electronics with the Energy Research Institute, NTU (ERI@N) and co-Director of the Rolls-Royce at NTU Corporate Lab, Singapore. From February 2001 to January 2002, and February 2005 to January 2006, he was a Researcher with the Center for Power Electronics Systems, Virginia Tech, Blacksburg, VA, USA. From January 2012 to January 2013, he was a Visiting Professor with the Australian Energy Research Institute, UNSW, Sydney. He has authored or coauthored more than 440 published technical papers and has been involved in several industrial projects and educational programs in the fields of power electronics and systems. His research interests include modulation and control of power converters, multilevel converters, renewable energy, energy storage, power quality, HVdc transmission systems, and more-electrical aircraft and vessels.

Dr. Pou was the recipient of the 2018 IEEE Bimal Bose Award for Industrial Electronics Applications in Energy Systems. He is Associate Editor for the *IEEE Journal of Emerging and Selected Topics in Power Electronics*. He was co-Editor-in-Chief and Associate Editor for the IEEE TRANSACTIONS ON INDUSTRIAL ELECTRONICS.

Georgios Konstantinou (Senior Member, IEEE) received the B.Eng. degree in electrical and computer engineering from the Aristotle University of Thessaloniki, Thessaloniki, Greece, and the Ph.D. degree in electrical engineering from UNSW Sydney (The University of New South Wales), Sydney, Australia, in 2007 and 2012, respectively.

From 2013 to 2016, he was a Senior Research Associate with the University of New South Wales, Sydney, NSW, Australia, where he was part of the Australian Energy Research Institute. Since 2017, he has been with the School of Electrical Engineering and Telecommunications, UNSW Sydney, where he is currently a Senior Lecturer. His main research interests include multilevel converters, power electronics in HVDC, renewable energy, and energy storage applications. He is an Associate Editor for IEEE TRANSACTIONS ON POWER ELECTRONICS.